Characterization of Inositol-1,4,5-Trisphosphate-Gated Channels in the Plasma Membrane of Rat Olfactory Neurons

Fritz W. Lischka,[#] M. Muz Zviman,[#] John H. Teeter,[#§] and Diego Restrepo*

*Department of Cellular and Structural Biology, University of Colorado Health Sciences Center, Denver, Colorado 80262; [#]Monell Chemical Senses Center, Philadelphia, Pennsylvania 19104; and [§]Department of Physiology, University of Pennsylvania, Philadelphia, Pennsylvania 19104 USA

ABSTRACT It is generally accepted that inositol-1,4,5-trisphosphate ($InsP_3$) plays a role in olfactory transduction. However, the precise mode of action of $InsP_3$ remains controversial. We have characterized the conductances activated by the addition of 10 μM $InsP_3$ to excised patches of soma plasma membrane from rat olfactory neurons. $InsP_3$ induced current fluctuations in 25 of 121 inside-out patches. These conductances could be classified into two groups according to the polarity of the current at a holding potential of +40 to +60 mV (with Ringer's in the pipette and pseudointracellular solution in the bath). Conductances mediating outward currents could be further divided into large- (64 $\pm$ 4 pS, $n = 4$) and small- (16 $\pm$ 1.7 pS, $n = 11$) conductance channels. Both small- and large-conductance channels were nonspecific cation channels. The large-conductance channel displayed bursting behavior at +40 mV, with flickering increasing at negative holding potentials to the point where single-channel currents were no longer discernible. The small-conductance channel did not display flickering behavior. The conductance mediating inward currents at +40 to +60 mV reversed at +73 $\pm$ 4 mV ($n = 4$). The current traces displayed considerable fluctuations, and single-channel currents could not be discerned. The current fluctuations returned to baseline after removal of $InsP_3$. The power density spectrum for the excess noise generated by $InsP_3$ followed a 1/*f* dependence consistent with conductance fluctuations in the channel mediating this current, although other mechanisms are not excluded. These experiments demonstrate the presence of plasma membrane $InsP_3$-gated channels of different ionic specificity in olfactory receptor cells.

INTRODUCTION

The existence of a plasma membrane inositol-1,4,5-trisphosphate ($InsP_3$)-gated nonspecific cation channel in vertebrate olfactory receptor neurons was first postulated on the basis of unitary current fluctuations induced by $InsP_3$ in catfish olfactory cilia membranes incorporated into an artificial lipid bilayer (Restrepo et al., 1990). Subsequent immunohistochemical (Cunningham et al., 1993; Kalinoski et al., 1993) and biochemical (Restrepo et al., 1992; Kalinoski et al., 1992) evidence indicated that an $InsP_3$-receptor protein is present in the plasma membrane of the apical compartments (cilia and olfactory knob) of vertebrate olfactory receptor neurons. Whole-cell patch-clamp measurements of the response of isolated olfactory neurons to cytoplasmic $InsP_3$ were consistent with the existence of $InsP_3$-modulated conductances in vertebrate olfactory neurons (Miyamoto et al., 1992a; Okada et al., 1994) but did not provide information on the mechanism of action (direct or indirect) of $InsP_3$. However, when combined with imaging of intracellular calcium concentration, whole-cell patch-clamp experiments provided substantial evidence, indicating that olfactory receptor neurons possess apical nonspecific cation and Ca^{2+}-permeable conductances modulated by $InsP_3$ (Schild et al., 1995; Kashiwayanagi, 1996).

Measurements with excised plasma membrane patches have conclusively demonstrated the presence of $InsP_3$-gated channels in the apical dendrite of lobster olfactory receptor cells (the morphological equivalent of the cilia of vertebrate olfactory receptor cells) (Fadool and Ache, 1992; Hatt and Ache, 1994). In lobster, $InsP_3$ is believed to be the second messenger mediating excitatory olfactory responses through the opening of dendritic $InsP_3$-gated cation channels, and cAMP is believed to mediate inhibitory responses by opening a cAMP-gated K^+ channel (Michel and Ache, 1992; Fadool and Ache, 1992; Michel et al., 1991; Hatt and Ache, 1994; Boekhoff et al., 1994). In vertebrates, however, several laboratories have failed to obtain responses upon dialysis of $InsP_3$ into the cytoplasm of olfactory receptor neurons (Lowe and Gold, 1993; Nakamura et al., 1994; Firestein et al., 1991). In addition, two laboratories have reported no effect of $InsP_3$ on currents recorded in excised patches from olfactory cilia membranes (Nakamura et al., 1996; Kleene et al., 1994).

Although a brief report of the presence of $InsP_3$-gated channels in excised patches from soma and olfactory knob of frog olfactory receptor cells has been published (Suzuki, 1994), it is clear that the existence of $InsP_3$-gated channels in the plasma membranes of vertebrate olfactory receptor neurons remains controversial (Firestein, 1996). To explore this question we have measured current fluctuations elicited by $InsP_3$ in excised patches of soma plasma membrane from rat olfactory receptor cells. We find that $InsP_3$ elicits current fluctuations that can be classified into three different groups

Received for publication 21 September 1998 and in final form 13 November 1998.

Address reprint requests to Dr. Diego Restrepo, Department of Cellular and Structural Biology, Campus Box B111, University of Colorado Health Sciences Center, 4200 East Ninth Ave., Denver, CO 80262. Tel.: 303-315-4715; Fax: 303-315-4729; E-mail: diego.restrepo@uchsc.edu.

0006-3495/99/03/1410/13 $2.00

on the basis of their reversal potentials, open channel noise level, and single-channel conductance and kinetics. The characteristics of these conductances are consistent with those of olfactory $InsP_3$-gated channels described in previous reports in vertebrates and invertebrates (Restrepo et al., 1990; Honda et al., 1995; Suzuki, 1994; Fadool and Ache, 1992; Hatt and Ache, 1994). The olfactory $InsP_3$-gated channels display both similarities and differences when compared to the $InsP_3$-gated channels found in internal membranes (endoplasmic reticulum (ER) and sarcoplasmic reticulum (SR); Watras et al., 1991). These experiments indicate that vertebrate olfactory receptor neurons possess different types of plasma membrane $InsP_3$-gated channels differing in ionic specificity and kinetics.

MATERIALS AND METHODS

Solutions

Dissociation solution contained (in mM) 145 NaCl, 5 KCl, 2 EDTA, 20 HEPES, 1 Na-pyruvate. Cells were maintained in standard Ringer's (in mM): 145 NaCl, 5 KCl, 2 $CaCl_2$, 1 $MgCl_2$, 20 Na-HEPES, 1 Na-pyruvate, 5 glucose. Standard Ringer's was also used as the pipette solution, which corresponds to the extracellular side of the inside-out patch. For the Ba-Ringer's, 5 mM $BaCl_2$ was added to the standard Ringer's and $CaCl_2$ was omitted.

The intracellular solution $I_{K\text{-}asp}$ contained (in mM) 145 K-aspartate, 1 $MgCl_2$, 0.4 $CaCl_2$, 1 EGTA 1, and 10 K-HEPES. In some records potassium was replaced by cesium ($I_{Cs\text{-}asp}$; indicated in the figure legends). All solutions had a pH of 7.2, adjusted with the hydroxide of the main cation, and an osmolarity of 300 mOsmol. Inositol 1,4,5-trisphosphate was added to the bath at concentrations of 3 or 10 μM. All salts, enzymes, and reagents were from Sigma (St. Louis, MO) unless otherwise stated.

Olfactory neuron isolation

Male Spraque-Dawley rats were sacrificed by exposure to 100% CO_2, and the olfactory tissue (posterior part of the septum and the turbinates of both sides) was removed. The tissue was cut into small pieces and incubated with dissociation solution containing 12 U/ml papain for 15 min. The suspension was triturated with a Pasteur pipette, and Ringer's solution with 10 μg/ml leupeptin (stop solution) was added. The cells were then filtered through a nylon mesh, and the solution was put onto a density gradient consisting of a bottom layer of Ringer's solution containing 40% Percoll and a top layer with 20% Percoll solution. The cells were centrifuged for 5 min at 400 rpm and then taken from the interface between the 40% and 20% solutions. Olfactory neurons were plated onto concanavalin A-coated slides and kept in a moist chamber at room temperature for up to 5 h.

Inside-out patch-clamp measurements

$InsP_3$-induced current fluctuations were measured in plasma membrane patches from rat olfactory neuron soma, using the inside-out configuration of the patch-clamp technique (Hamill et al., 1981). The recording setup consisted of an inverted microscope (Zeiss IM 35) on which the recording chamber was mounted. For the recordings a patch-clamp amplifier (Axopatch 200A; Axon Instruments) was used. The data were low-pass-filtered with a 1-kHz Bessel filter and were digitized at 5 or 10 kHz with a DigiData 1200 interface (Axon instruments).

Patch pipettes were pulled from borosilicate glass (Corning 7052; World Precision Instruments, Sarasota, FL) with a vertical puller (Narishige, Tokyo, Japan) and fire polished to a final resistance of 10–15 MΩ with the standard solutions. After a gigaohm seal (>10 GΩ) was obtained, an inside-out patch was excised by crossing the bath-air interface briefly. Some inside-out patches showed spontaneous channel activity, which in most cases faded away. Patches that showed sustained activity were not used for recordings. After a control trace was recorded, the membrane patches were exposed to the intracellular solutions containing $InsP_3$. Solutions were exchanged by replacement of the solution in the recording chamber. Complete exchange of solutions occurred within 1–5 min. The onset and the washout of the responses to $InsP_3$ occurred within this time frame. Because we were concerned with differentiating between a nonspecific cation conductance and a conductance that reversed at positive potentials (the rapidly fluctuating conductance; see below), most of the measurements of $InsP_3$-induced current fluctuations were at positive holding potentials (+40 to +60 mV). The rapidly fluctuating conductance was not measured at negative holding potentials, because under these conditions the patches often became unstable.

Data analysis

The $InsP_3$-induced current fluctuations were characterized using the mean-variance histogram method of Patlak (1993). Briefly, the mean ($\langle I \rangle$) and the variance (s^2) of the current were calculated within a sliding window containing W data points. The mean-variance estimates were then binned into a two-dimensional histogram (the mean-variance histogram). The x and y dimensions for the mean-variance histogram were the mean current and the logarithm of the variance, respectively (divided into 96 bins each), and the z axis was the logarithm of the number of points falling within each mean-variance bin. Figs. 1 *A*, 2 *A*, 3 *A*, and 4 *A* show representative traces of $InsP_3$-activated currents, and Figs. 1 *B*, 2 *B*, 3 *B*, and 4 *B* show the corresponding mean-variance histograms computed with a window width (W) of 5 points. In these figures, the z axis value in each bin was represented with a gray tone. As discussed in detail by Patlak (1993), the topology of the mean-variance histogram reflects the kinetics of the current fluctuations. Closed and open states are represented by low variance peaks such as those with peak mean at 0 pA and peak variance at 0.009 pA^2 for the closed level and 0.85 pA and 0.018 pA^2 for the open level in Fig. 3 *B*. The transitions between states are represented by the arches bridging the low variance peaks.

To estimate mean open channel current and the fraction of the time that the channels were open (F_o), we fit the low variance peak corresponding to the closed state with the product of a Gaussian function and a χ^2 distribution (Gaussian-χ^2 Squared envelope function) (Patlak, 1993):

$$N_{mv} = V_{mv} B_v P_v(s^2) B_m P_m(\langle I \rangle) \quad (1)$$

where N_{mv} is the amplitude of any single bin mv, B_m and B_v are the binwidths for the mean and variance distributions, respectively, and

$$P_m(\langle I \rangle) = \frac{1}{2\pi\sigma^2} e^{(((I)-\mu)/2\sigma^2)} \quad (2)$$

$$P_v(s^2) = (n/\sigma^2)(2^{n/2}\Gamma(n/2))^{-1}(ns^2/\sigma^2)^{[(n/2)-1]} e^{(-ns^2/2\sigma^2)} \quad (3)$$

where μ is the population mean, σ^2 is the variance of the distribution of $\langle I \rangle$ around μ, and n is the number of degrees of freedom. The best-fitting volume was then subtracted from the mean-variance histogram, and the mean open current was estimated as the mean current of all data points after subtraction of the closed state. The fraction of the time that the channel was open was estimated as the volume of the histogram after subtraction of the closed-state peak divided by the total number of data points in the record.

To estimate chord conductances, open-channel current levels were determined by fitting the low-variance peaks for the closed and open states with Eq. 1. In a few cases, fast transitions severely affected the estimation of the open-channel current level (Silberberg and Magleby, 1993). However, even in these records long dwell-time openings were found that could be used to calculate the chord conductance accurately. For these records, an idealized trace was constructed according to the algorithm of Zviman and

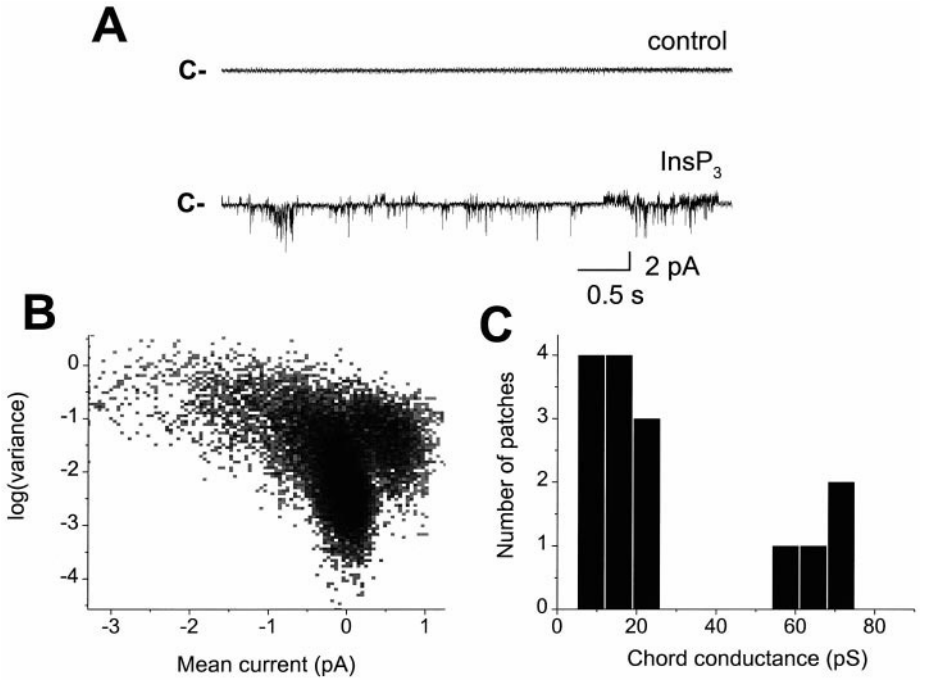

FIGURE 1 Among a total of 25 patches responsive to $InsP_3$, two patches exhibited both inward and outward current fluctuations, whereas all other patches responded with either inward or outward current fluctuations at holding potentials between +40 and +60 mV. (*A*) Example of inward and outward current fluctuations elicited by the addition of 10 μM $InsP_3$ in a soma membrane patch at a holding potential of +60 mV. Current traces before (control) and during ($InsP_3$) perfusion with 10 μM $InsP_3$ are shown. Pseudointracellular solution was supplemented with 5 mM $BaCl_2$ in this experiment. (*B*) Mean-variance histogram with a window size of five points for the trace shown in *A* after the addition of $InsP_3$. The number of points with mean and variance falling within each bin is denoted by a 32-step logarithmic gray scale (white = 1, black = 125). The low variance peak for the closed state had a peak mean current of 0 pA and a variance of 0.0065 pA^2. The outward current fluctuations had a peak mean current of 0.57 pA and a variance of 0.05 pA^2. The inward current fluctuations did not display a defined low variance peak. (*C*) Histogram of chord conductance values, calculated at either +40 or +60 mV, for outward current fluctuations elicited by $InsP_3$ in patches from rat olfactory neuron soma plasma membrane. The number of patches responding with an outward current was 15. The abscissa represents the number of patches with chord conductances falling within each given conductance range (binwidth 7 pS).

co-workers (Restrepo et al., 1996b). A plot of current amplitude versus logarithm of the dwell time was constructed, and the open current levels were obtained from estimates of openings with long dwell times. For the calculation of the chord conductance (Fig. 1 *C*), it was assumed that the reversal potential was −11.7 mV for the small channels and −19 mV for the large conductance channels (see below in Results).

A program ("levels") was written in Borland C++ to perform these calculations. The program reads the raw data in Axon ABF format, displays the data, and allows the user to construct and display a mean-variance histogram for any portion of the record, to perform trace idealization, and to determine the power density spectrum of the trace. The low variance peaks in the mean-variance histogram are automatically fit to Eq. 1, using a Levenberg-Marquadt algorithm (Press et al., 1992), as detailed by Patlak (1993). The program also calculates histogram volumes in arbitrary regions of interest for varying window widths (*W*). This feature of the program was used to estimate the window width dependence of low-variance volumes (Figs. 2*F*, 3 *D* and *E*, and 4 *F*). (Levels is available in 32-bit format for Windows 95 or NT at URL http://www.uchsc.edu/ctrsinst/rmtsc/restrepo/index.html.) We find that, compared to half-amplitude thresholding methods (Dempster, 1993; Sakmann and Neher, 1995), the mean-variance histogram technique provided a fast, objective method for analyzing large amounts of single-channel data.

Noise analysis (DeFelice, 1981) was implemented according to algorithms published by Dempster (Dempster), using the fast Fourier transform code in *Numerical Recipes in C* (Press et al., 1992). Levels allowed construction of power density spectra in the considerable range from 0.03 to 1000 Hz, using a 131,072-point fast Fourier transform. The data were multiplied by a Welch window to limit leakage at high frequencies (Press et al., 1992; Dempster, 1993). Power density spectra in the absence of $InsP_3$ were subtracted from density spectra in the presence of $InsP_3$ to estimate the power density distribution of the excess noise generated by the addition of $InsP_3$ (Fig. 4 *E*).

RESULTS

$InsP_3$ regulates three different plasma membrane conductances

We recorded from a total of 121 inside-out patches excised from the soma of rat olfactory receptor cells. Thirty-one of these patches displayed spontaneous current fluctuations, which were due to the presence of K^+ channels in the patch, as evidenced by the fact that replacement of Cs^+ for K^+ in the bath abolished spontaneous channel activity ($n = 3$) and that recordings in the presence of Cs^+ in the bath did not display spontaneous fluctuations ($n = 9$). Of the remaining 71 patches, 25 responded to the addition of 10 μM inositol-1,4,5-trisphosphate to the bath (cytoplasmic side) with an increase in membrane conductance. Analysis of the responses to $InsP_3$ indicated that three different conductances were modulated by $InsP_3$ in these patches.

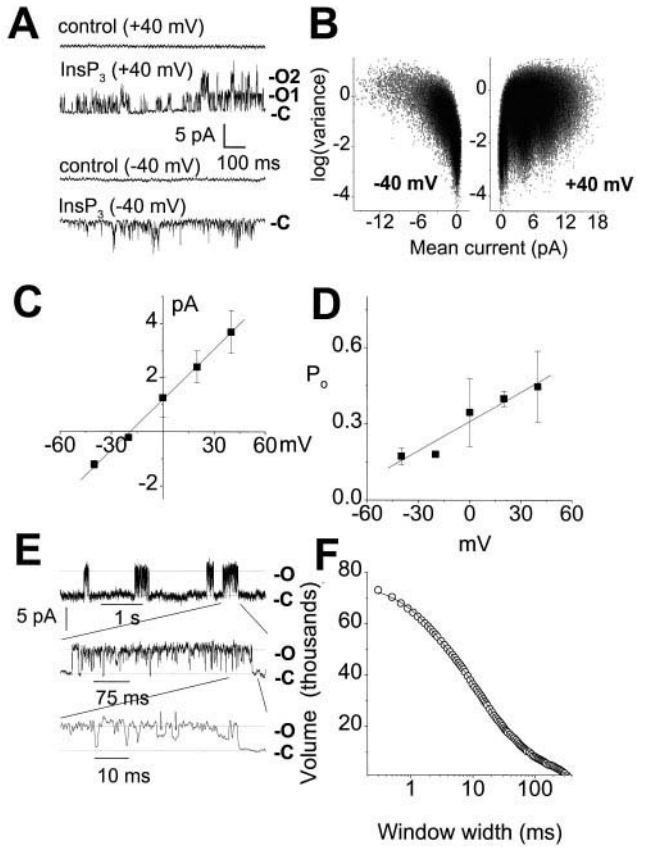

FIGURE 2 Characteristics of the current fluctuations mediated by large-conductance nonspecific cation channels activated by $InsP_3$ in plasma membrane patches from the soma of rat olfactory neurons. (*A*) Traces displaying currents recorded before (control) and during ($InsP_3$) exposure to 10 μM $InsP_3$ at holding potentials of +40 and −40 mV. The patch contained two channels. C, O1, and O2 denote closed and open levels one and two, respectively. Notice that at +40 mV single-channel openings were clearly defined, but at −40 mV single-channel openings could not be discerned. (*B*) Mean-variance histogram with a window of five points for a 30-s record measured in the same patch. The number of points with mean and variance falling within each bin is denoted by a 32-step logarithmic gray scale (for +40 mV: white = 1, black = 400; for −40 mV: white = 1, black = 1260). A fit of Gauss-χ^2 envelope functions to the peaks in the histogram at +40 mV yielded mean currents and variances of 0 pA and 0.009 pA^2 for the closed state, 3.2 pA and 0.23 pA^2 for the first open level, and 6.2 pA and 0.55 pA^2 for the second open level. The histogram at −40 mV did not display well-defined open-level low-variance peaks. (*C*) Dependence of mean open current on holding potential. The mean open current was estimated as described in Materials and Methods. The current for the closed state was subtracted from the absolute current level before the estimation of the mean open current. The number of independent determinations for mean open current at the different holding potentials was +40 mV (4), +20 (3), 0 (2), −20 (1), and −40 (3). Linear regression yielded a reversal potential of −19 mV and a slope conductance of 62 pS. (*D*) Dependence of the open probability (P_o) on membrane potential. The line shown is a linear regression of the data, with a slope of 0.004 mV^{-1} and an intercept of 0.31. The number of independent determinations at each holding potential is the same as in *C*. (*E*) Example of a section of a record that displayed only one channel opening (the holding potential was +40 mV). This patch contained two large conductance channels, as evidenced by the fact that two openings were detected elsewhere. Openings occurred in bursts. Two successive time-scale amplifications are shown for a section of the trace that included a burst of openings. Current excursions from the open level to an intermediate level are found within the burst (*arrows*). O and C denote open and closed current levels, respectively. (*F*) Dependence of the volume in the low variance region corresponding to the open level for the record in *E* on window width (in ms). The solid line was determined by a least-squares fit of the sum of three exponentials with time constants of 2, 15, and 130 ms. Low-variance region volumes for the open state calculated within four regions of the trace where only one opening was evident were added to produce the data shown in the graph.

Fig. 1 illustrates the basis for classification of these conductances into three different groups. When the membrane potential was held between +40 and +60 mV, addition of $InsP_3$ to the cytoplasmic side of the patch induced outward as well as inward current fluctuations. An example is displayed in Fig. 1 *A*, which shows a patch that responded to $InsP_3$ with both inward and outward current fluctuations at a holding potential of +60 mV. Fig. 1 *B* displays the mean variance histogram for the record in Fig. 1 *A*. The MV histogram shows that the inward current fluctuations do not settle on a low-variance open state indicative of high open-channel noise (see below). Most patches (23 of 25) responded with either inward (n = 10) or outward (n = 13) current fluctuations. The example in Fig. 1 *A* is only shown to illustrate the fact that the conductances that mediated the inward and outward current fluctuations at positive holding potentials were occasionally found in the same patch (2 of 25 patches).

The $InsP_3$-activated conductances mediating outward current fluctuations at positive holding potentials could be further classified into two categories according to the magnitude of the single-channel conductance (Fig. 1 *C*). As a result, for the purpose of analyzing the data, we classified the records among three groups: those displaying inward currents in the holding potential range from +40 to +60 mV (12 patches), and small and large conductance channels mediating outward currents. Of 15 patches displaying outward currents, 11 patches contained small conductance channels and four possessed large conductance channels. As shown below, within these groups the $InsP_3$ conductances exhibited homogeneous behavior in terms of reversal potentials, single-channel kinetics, noise properties, and pharmacology. Small (27–37 pS) and large (64–103 pS) conductance $InsP_3$-gated nonspecific cation channels, which carry outward currents at +40 to +60 mV, have previously been described in excised dendrite patches from lobster olfactory neurons (Fadool and Ache, 1992; Hatt and Ache, 1994), and in studies of rat and catfish olfactory cilia incorporated into an artificial bilayer at the tip of a patch pipette (Restrepo et al., 1990; Honda et al., 1995).

Large conductance nonspecific cation channels

The average chord conductance for the large conductance nonspecific cation channels was 64 ± 4 pS (mean ± SEM, n = 4) (Fig. 1 *C*, Table 1). Fig. 2 *A* shows a recording from a patch containing two large conductance channels, and Fig. 2 *B* shows the corresponding mean-variance histograms. As shown in the figure, the current reversed when the holding potential was switched from +40 mV to −40 mV. Fig. 2 *C*

shows the current-voltage relationship for mean open current averages from four records. The average reversal potential estimated from data from three independent experiments was -19 ± 4 mV (mean $\pm$ SEM, $n = 3$) with $I_{K\text{-asp}}$ solution in the bath and Ringer's or Ba-Ringer's in the pipette. The presence/absence of 5 mM $BaCl_2$ in the pipette did not produce a substantial shift in the reversal potential (not shown). Although the ionic dependence of the channel was not investigated in detail, these data suggest that the channel is a nonspecific cation channel, because under these conditions the reversal potential for monovalent ions was $E_{Na} = +\infty$, $E_K = -87$ mV, and $E_{Cl} = -103$ mV.

The open probability and the open channel noise of the large conductance channel were voltage dependent. Fig. 2 *A* illustrates the fact that the open-channel noise level increased when the membrane potential became negative. Thus, whereas at +40 mV two current levels could be clearly discerned, at −40 mV the open-current levels could not easily be discerned because of an increase in noise. This increase in noise is reflected by the lack of low variance peaks for the open state in the mean-variance histogram at −40 mV, contrasting with the mean-variance histogram at +40 mV, which displays two low variance regions corresponding to two open-current levels at 3.2 and 6.2 pA (Fig. 2 *B*).

Fig. 2 *B* also illustrates the fact that the large conductance channel spent a larger fraction of the time in the open state at positive holding potentials. Because the patches included multiple channels, the open probability (P_o) for the large conductance channel could not be calculated directly. However, an estimate of P_o was obtained by assuming that channel openings occurred following binomial statistics. For a binomial system with n independent units, P_o can be calculated using the equation (Jorquera et al., 1995)

$$P_o = 1 - (F_c)^{(1/n)} \quad (4)$$

where F_c is the fraction of the time that the channel spends in the fully closed state, which could be estimated by fitting the volume under the closed state of the mean-variance histogram with the Gaussian-χ^2 envelope function (see Materials and Methods). Fig. 2 *D* shows the dependence of open probability, estimated using Eq. 1, on membrane potential. As shown, P_o increases as the membrane is depolarized. A change of 70 mV is necessary to increase the open probability by *e*-fold, suggesting that 0.7 effective charges must cross the electric field to open the channel (Sigworth, 1995). The $InsP_3$-gated channel of rat cerebellar endoplasmic reticulum (Watras et al., 1991) and the large conductance $InsP_3$-gated channel of lobster olfactory neurons (Hatt and Ache, 1994) also exhibit a weak dependence of P_o on holding potential. In contrast, 12 charges are involved in opening the activation gate of the skeletal muscle voltage-gated sodium channel (an *e*-fold increase takes place in 2.2 mV) (Hirschberg et al., 1995).

Closed dwell-time kinetics could not be studied in these records because of the presence of multiple channels in each patch. However, it was possible to find long periods of time (>5 s) with only one channel opening in one of the records (Fig. 2 *E*). As shown in the figure, openings at positive holding potentials were characterized by bursts lasting up to 1 s. During the bursts the channel displayed "flickering" behavior, and occasionally the current level decreased to intermediate current levels indicative of subconductance levels (Fig. 2 *E*, *arrows in lower trace*). Often the channel was observed in a level half way between the fully open and closed states. However, subconductance levels of ¼ and ¾ of the full conductance level were also observed, but their amplitude could not be quantified rigorously because the subconductance levels did not form clear peaks in amplitude or mean-variance histograms because of the high level of open-channel noise. Intermediate levels were observed in all measurements from patches containing large conductance channels.

To quantify the time constants characterizing the duration of the bursts and the duration of "flickery" openings occurring within the bursts, we determined the dependence of the volume of the low variance region representing the open state in the mean-variance histogram on the width of the window used to calculate the mean and the variance. According to Patlak (1993), a plot of the low variance region volume versus window size is equivalent to a dwell-time histogram constructed from an idealized trace and can therefore be used to determine the time constants characterizing the kinetics of the open state. These data were fit by a sum of three exponentials (*solid line* in Fig. 2 *F*) with time constants of 2, 15, and 130 ms. The longest time constant (130 ms) characterizes the kinetics of the bursts, and the two short time constants (2 and 15 ms) characterize the open times for the flickering that occurs within the bursts. Similar analysis from two other records substantiated the fact that the open-time histogram was fit by multiple exponentials. However, in these two records, the sections of the trace that displayed only one opening were brief (<1 s), precluding a rigorous determination of the long time constant. The average estimates for the time constants from the three records analyzed were (mean $\pm$ SEM (n)): $t_1 = 1.6 \pm 0.3$ (3), $t_2 = 12.6 \pm 1.2$ (3), and $t_3 = 64$–130 (2) ms.

Small conductance nonspecific cation channels

The average chord conductance for the small conductance nonspecific cation channels was 16 ± 1.7 pS (mean $\pm$ SEM, $n = 11$) (Fig. 1 *B*, Table 1). Fig. 3 *A* shows a record of $InsP_3$-induced current fluctuations occurring in a patch containing a small conductance channel at a holding potential of +60 mV, and Fig. 3 *B* shows the corresponding mean-variance histogram. As shown in the figure, most of the openings were to a level of 0.85 pA, corresponding to a chord conductance of 12 pS in this record. Occasionally, a channel opened to a level with twice the conductance of the main level (see *arrow* in Fig. 3 *A*, expanded below), suggesting that the channel could open to a second conductance

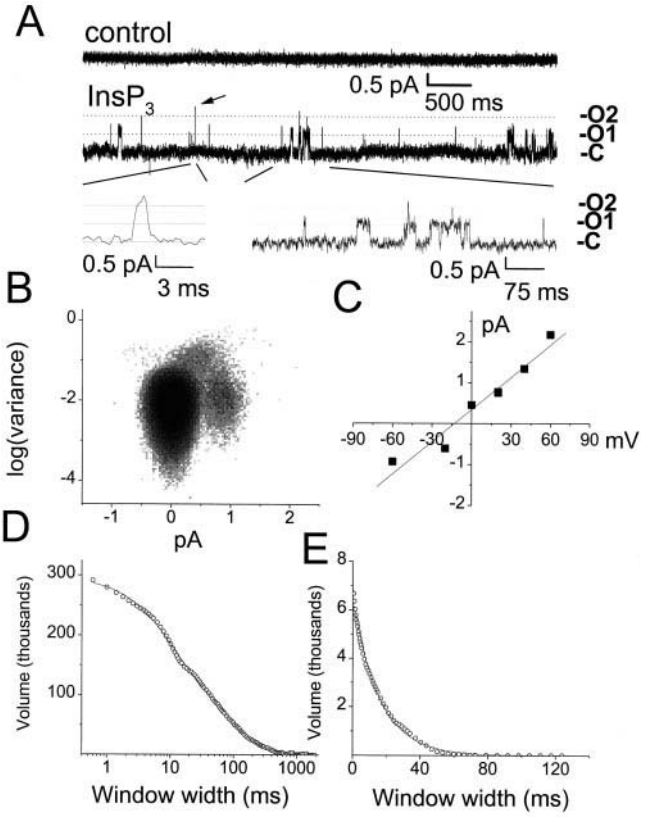

FIGURE 3 Characteristics of the current fluctuations mediated by small-conductance nonspecific cation channels activated by $InsP_3$ in plasma membrane patches from the soma of rat olfactory neurons. (*A*) Traces displaying currents recorded before (control) and during ($InsP_3$) exposure to 10 μM $InsP_3$ at a holding potential of +60 mV. Openings could be resolved to two different levels. C, O1, and O2 denote closed and open levels one and two, respectively. (*B*) Mean-variance histogram for the entire 30-s record that included the trace in *A*. The number of points with mean and variance falling within each bin is denoted by a 32-step logarithmic gray scale (white = 1, black = 2000). A fit of a Gauss-χ^2 envelope function of the low variance peaks for the closed and open states yields values for peak mean current and variance of 0 pA and 0.009 pA^2 for the closed level and 0.85 pA and 0.018 pA^2 for the open level. (*C*) Relationship between mean open current and membrane potential for one patch containing a small-conductance channel. The pipette contained BaRinger's, and the bath contained Kasp solution. A linear regression (*solid line*) yielded −11.7 mV for the reversal potential and 26 pS for the slope conductance. (*D* and *E*) Dependence of volume of low variance components of mean variance histograms for trace in *A* on window width. (*D*) Dependence of low variance component volume for the open state on window width (in ms). The solid line is an exponential with a time constant of 16 ms. (*E*) Dependence of low variance component volume for the closed state on window width (in ms). The solid line is the sum of three exponentials with time constants of 8, 61, and 260 ms.

level. Excursions to a second conductance level were observed in 6 of 14 patches with small conductance channels. Openings to the second level were rare (as can be seen in the histogram in Fig. 3 *B*) and did not obey binomial statistics (not shown), indicating that the openings to the second level were not due to simultaneous opening of two channels. The fact that openings to the second level were never observed independently suggests but does not prove conclusively that the openings to the higher conductance levels were openings to a higher subconductance level exhibited by the same channel that displayed the 16-pS openings. There were also excursions to a second conductance level of 37 pS of the small conductance channel studied in isolated rat olfactory cilia incorporated into artificial bilayers (Honda et al., 1995). However, in that case the second level was the main level, and excursions to the first level were brief (t_{open} of 4.5 ms), whereas excursions to the second level were long (t_{open} of 88 ms). We do not know why there was such a difference in level occupancy between the two sets of experiments, but it is likely that reconstitution of the membrane results in alteration of the kinetics of the channel.

Fig. 3 *C* shows the current-voltage relationship for one small conductance channel recorded with $I_{K\text{-}asp}$ solution in the bath and Ba-Ringer's in the pipette. The reversal potential was −11.7 mV, suggesting that the channel was a nonspecific cation channel. The ionic dependence of the current-voltage relationship was not investigated further.

Seven patches contained only one small conductance channel. As shown in Fig. 3 *A*, in contrast to the large conductance channel, the small conductance channel did not burst. An analysis of the kinetics of the small conductance channel was undertaken by determining the dependence of the volume in the low variance components of the mean variance histogram as a function of window width at +60 mV holding potential (Fig. 3, *D* and *E*). The dependence of the volume of the low variance component on window width for the open state could be fit by a single exponential with a time constant of 25.7 ± 6 ms (mean ± SEM, $n = 7$), with three of the records displaying a second exponential component with a time constant of 165 ± 79 ms (mean ± SEM, $n = 3$) (Fig. 3 *D*), whereas the dependence for the closed state was fit by a function with two- or three-exponential components with time constants (mean ± SEM (n)) of 12.9 ± 0.8 (7), 83 ± 14(4), and 400 ± 54(7) ms. The open probability at +60 mV holding potential was 0.13 ± 0.03 (mean ± SEM, $n = 7$). The dependence of the kinetics of the small conductance channel on voltage was not investigated in detail.

Rapidly fluctuating $InsP_3$-gated conductance

Fig. 4 *A* shows the current recorded from an excised patch at a holding potential of +60 mV before and after the addition of 10 μM $InsP_3$, and Fig. 4 *B* shows the corresponding mean variance histogram. In this patch $InsP_3$ elicited inward current fluctuations that did not display the discrete current levels typically found in single-channel records (see enlarged time scale in Fig. 4 *A*). This was further evidenced by the lack of a defined low variance region for the open state in the mean variance histogram (Fig. 4 *B*).

Because such rapid current fluctuations could be due to seal breakdown, we studied the characteristics of the inward current in detail. Five independent observations indicate

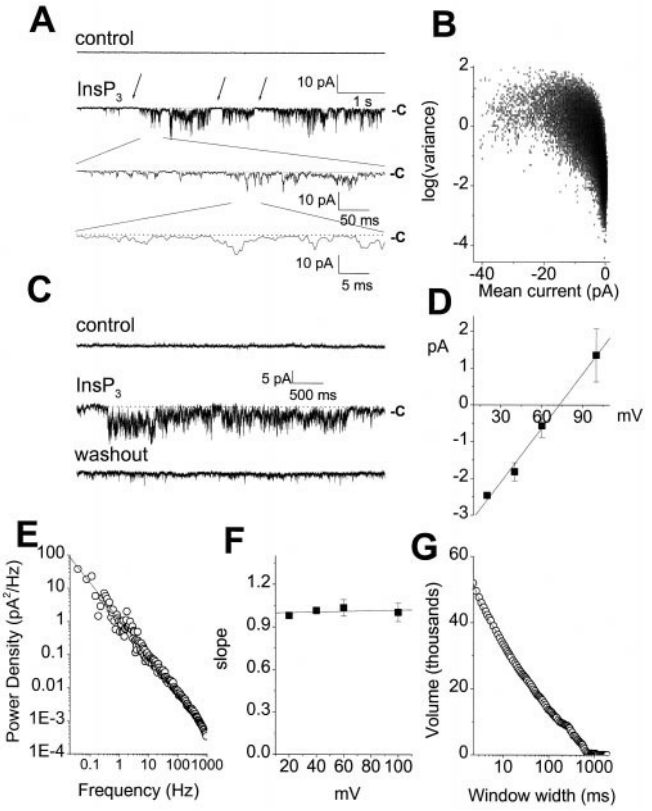

FIGURE 4 Characteristics of the $InsP_3$-activated conductance mediating inward currents at +40 to +60 mV. (*A*) Traces displaying currents recorded before (control) and during ($InsP_3$) exposure to 10 μM $InsP_3$ at a holding potential of +60 mV. $InsP_3$ elicited inward current fluctuations from a closed level (C), but no clear channel-like openings could be discerned. Notice the presence of silent periods in the record (*arrows*). (*B*) Mean-variance histogram for the entire 30-s record that included the trace in *A*. The number of points with mean and variance falling within each bin is denoted by a 32-step logarithmic gray scale (white = 1, black = 2000). A fit of a Gauss-χ^2 envelope function of the low variance peak for the closed state yields values for peak mean current and variance of 0 pA and 0.027 pA^2. Notice that a low variance component for the open state is not apparent. (*C*) Reversibility of the $InsP_3$-activated inward current (holding potential +60 mV). The figure shows traces before (control), during ($InsP_3$), and 1 min after (washout) perfusion with 10 μM $InsP_3$. (*D*) Dependence of mean open current on membrane potential for the $InsP_3$-activated conductance mediating inward currents at +40 to 60 mV. The data are from the following number of independent determinations: +100 mV (3), +60 mV (2), +40 mV (4), +20 mV (1). The solid line is a least-squares best-fit line with reversal potential 72.7 mV and a slope conductance of 49 pS. (*E*) Power density spectrum for the excess noise generated by the addition of $InsP_3$ in the record shown in *A*. A 131,072-point fast Fourier transform was used. The data are fit with a straight line with a slope of −1.1. (*F*) Slope of the power density spectrum as a function of holding potential. A 32,768-point Fourier transform was used. The number of independent determinations at each holding potential was +100 mV (3), +60 mV (4), +40 mV (4), +20 mV (1). (*G*) Volume of the low variance peak volume for the closed state for the record in *A* as a function of window width (in ms). The solid line is the best fit of a sum of three exponentials with time constants of 1.4, 17, and 273 ms.

that the rapidly fluctuating inward currents are not an artifact, but rather represent an $InsP_3$-regulated conductance. First, we found that when a patch that responded to $InsP_3$ with a rapidly fluctuating inward current was washed with Ringer's solution, the inward current disappeared (Fig. 4 *C*, representative of three independent experiments). Seal breakage usually becomes worst upon washout due to mechanical disturbance of a weak seal. Second, the current-voltage relationship for this conductance reversed at 73 ± 4 mV (mean ± SEM, $n = 4$), demonstrating that the conductance is not a nonspecific cation conductance (Fig. 4 *D*, Table 1). Third, the inward current records displayed long periods where the variance of the current was equal to the variance in the absence of $InsP_3$ (Fig. 4 *A*, *arrows*). The presence of these "shut" stretches is consistent with a conductance that spends a significant fraction of the time in a closed state, not with seal breakdown whose resistance decreases monotonously as a function of time. Shut periods are found in excised patch current measurements of other rapidly fluctuating conductances (e.g., Chan et al., 1996; Hirschberg et al., 1995; Larsen et al., 1996; Hosoya et al., 1996; Gomez and Nasi, 1996). Fourth, rapidly fluctuating currents with characteristic shut periods were never detected before the addition of $InsP_3$ (121 of 121 records). Current fluctuations in spontaneously active patches (presumably K^+ channels) displayed typical single-channel openings. Finally, the addition of 10 μg/ml heparin decreased the open probability and reduced the mean open current by ~50% (Fig. 5).

To obtain information on the nature of the conductance(s) underlying the $InsP_3$-induced rapidly fluctuating inward current, we studied the properties of the excess noise generated by the addition of $InsP_3$. Fig. 4 *E* shows the power spectrum for records in Fig. 4 *A*. The spectrum is well fit by a line with a slope of −1.1 in the range of 0.03–1000 Hz, indicating that the process underlying the inward current has the characteristics of 1/*f* noise (DeFelice, 1981). The excess noise generated by $InsP_3$ in all patches displaying $InsP_3$-activated inward currents at positive potentials followed a 1/*f* dependence regardless of the holding potential (Fig. 4 *F*). Although other mechanisms are not excluded, the 1/*f* dependence, which has been reported for a variety of biological processes (DeFelice, 1981), is compatible with a channel that undergoes conductance fluctuations (DeFelice, 1981; Neher and Stevens, 1977), or with a channel with a dispersion in activation energies caused by the existence of multiple conformational substates (Dewey and Bann, 1992).

The presence of "shut" periods in the current traces recorded from patches that responded to $InsP_3$ with rapidly fluctuating inward currents at positive holding potentials indicated that the current was not generated by many independent channels opening at random. As shown in Fig. 4 *A*, the $InsP_3$-induced inward currents displayed long "shut" periods, sometimes as long as 1.5 s. The presence of these silent periods was detected in the mean variance histogram (Fig. 4 *B*) as a single low variance peak, and the kinetics of this "closed state" could be investigated by determining the dependence of the volume under the low variance peak on the size of the window used to calculate the mean and variance (Patlak, 1993). Such a plot indicates that the kinetics of the closed state can be fit by a sum of three

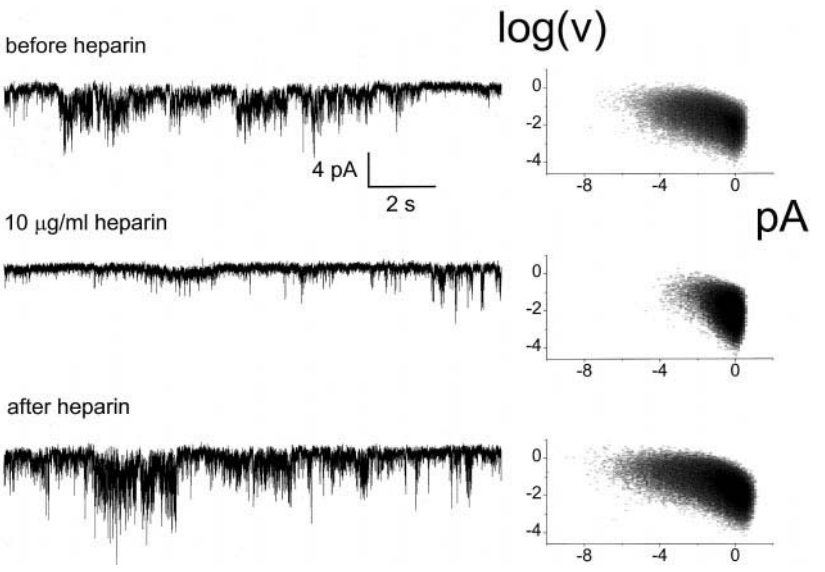

FIGURE 5 Effect of 10 μg/ml heparin on rapidly fluctuating InsP$_3$-activated conductance. Holding potential, +40 mV. Traces are representative of two independent experiments. Mean-variance histograms corresponding to each trace are shown on the right. The mean open currents (pA) and open probability calculated from the mean-variance histogram for the different conditions were −1.7, 0.5 before heparin; −0.65, 0.28 during heparin; and −1.45, 0.5 after heparin.

exponentials with time constants 1.4, 17, and 273 ms. The presence of this closed state is inconsistent with a model in which InsP$_3$ opens many independent channels, because such a system would follow binomial statistics, and the probability that all channels stay in the closed state for long periods of time would be small. The data are consistent with a channel that undergoes conductance fluctuations (Sigworth, 1986) or with many independent channels with low conductance that open cooperatively (i.e., their kinetics are not independent) (Larsen et al., 1996).

Inhibition by ruthenium red

Fig. 6 illustrates the effect of ruthenium red on the three types of InsP$_3$-activated conductances. Consistent with the known effects on olfactory InsP$_3$-gated nonspecific cation channels (Restrepo et al., 1990; Fadool and Ache, 1992; Honda et al., 1995; Suzuki, 1994; Restrepo et al., 1992), 10 μM ruthenium red abolished channel activity of both the large (Fig. 6, *A* and *D*) and small (Fig. 6, *B* and *D*) conductance nonspecific cation channels. In contrast, ruthenium red enhanced current fluctuations in those patches where InsP$_3$ induced an inward current at holding potentials of +40 to 60 mV (Fig. 6, *C* and *D*). Ruthenium red did not alter the 1/*f* dependence of the power density spectrum for the excess noise generated by the addition of InsP$_3$ in these records (not shown).

Effect of ionomycin

The rapidly fluctuating InsP$_3$-gated conductance described in this study reverses at +70 mV and does not display discernible single-channel openings. These properties are similar to those displayed by the conductance activated in some nonneuronal cells by release of Ca^{2+} from internal stores (I_{crac}) (Hoth and Penner, 1993; Zweifach and Lewis, 1993; Fanger et al., 1997). To determine whether the rapidly fluctuating InsP$_3$-gated conductance of rat olfactory cells was triggered by release of Ca^{2+} from internal stores that might have been included in the excised patches, we studied the effect of ionomycin on current fluctuations. Ionomycin is an electroneutral $Ca^{2+}/2H^+$ exchanger that has been used by Hoth and Penner (1993) to induce I_{crac}. We did not use thapsigargin to release Ca^{2+} from internal stores because in previous studies with rat olfactory neurons we had found that internal Ca^{2+} stores in these cells were not uniformly sensitive to thapsigargin (FitzGerald et al., 1993).

As shown in Fig. 7, ionomycin (5 μM) did not induce current fluctuations in excised patches from rat olfactory receptor neuron plasma membranes that exhibited InsP$_3$-activated current fluctuations (representative of four independent experiments). This happened even in a patch that responded to InsP$_3$ with rapidly fluctuating inward currents at +60 mV. These experiments indicate that the InsP$_3$-activated current fluctuations described in this study are not activated by depletion of Ca^{2+} from internal stores.

DISCUSSION

Plasma membrane InsP$_3$-gated channels have been postulated to mediate the response of olfactory neurons to some odorants (see Schild and Restrepo, 1998; Bruch, 1996; Restrepo et al., 1996a, for reviews). However, this hypothesis has been called into question because of the lack of an effect of InsP$_3$ on plasma membrane conductances in whole-cell or excised cilia patch-clamp experiments (Nakamura et al., 1994, 1996; Lowe and Gold, 1993; Firestein et al., 1991; Kleene et al., 1994). The lack of conclusive evidence for plasma membrane InsP$_3$-gated channels in vertebrate olfactory neurons has been cited as one of the major difficulties with the hypothesis that InsP$_3$ plays a mediatory role in olfactory transduction (Firestein, 1996). The experiments presented in this manuscript present strong evidence for InsP$_3$-gated channels in the plasma membrane

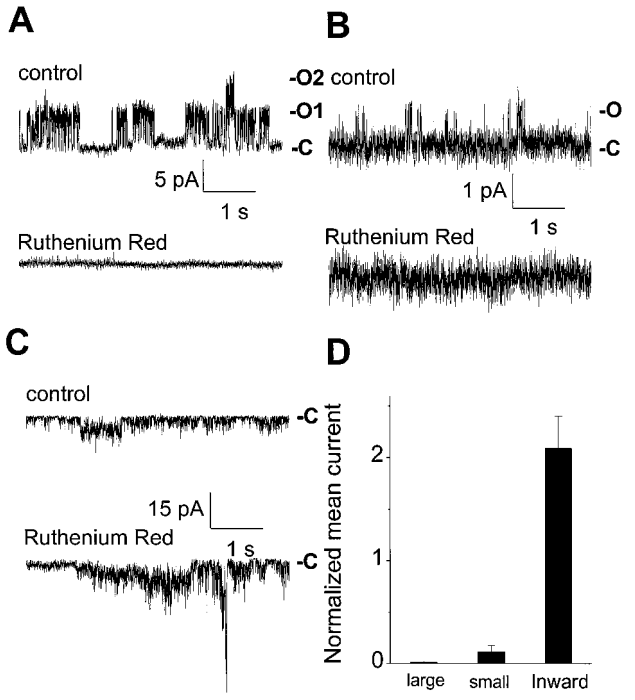

FIGURE 6 Effect of ruthenium red on $InsP_3$-activated conductances. (*A* and *B*) Ruthenium red (10 μM) inhibits the large (*A*) and small (*B*) conductance nonspecific $InsP_3$-activated channels. Holding potentials: +40 mV (*A*), +60 mV (*B*). (*C*) Ruthenium red enhances $InsP_3$-activated inward current at a holding potential of +60 mV. Traces are representative of three independent experiments. (*D*) Effect of ruthenium red on $InsP_3$-activated conductances. The mean current was calculated in each record from the absolute current levels in the presence of $InsP_3$ with or without ruthenium red after subtraction from each sample of the value of the mean current of the closed state. Mean current was normalized by dividing the value of the mean current after the addition of ruthenium red by the value of the mean current before the addition of ruthenium red (both in the presence of $InsP_3$). Holding potentials were in the range of +20 to +60 mV. Data shown are mean ± SEM (n = 3).

of rat olfactory neurons. We found three different conductances activated by $InsP_3$ in excised patches from soma plasma membrane: two nonspecific cation channels with conductances of 16 and 64 pS, and a rapidly fluctuating $InsP_3$-activated conductance that reversed at +74 mV in the presence of Ringer's solution in the pipette and pseudointracellular solution in the bath (Table 1). The small and large nonspecific cation channels have conductance levels, flickery bursting behavior, and pharmacology consistent with $InsP_3$-gated channels found in the dendrite of lobster olfactory neurons (Fadool and Ache, 1992; Hatt and Ache, 1994), rat and catfish olfactory cilia membranes reconstituted on artificial lipid bilayers (Restrepo et al., 1990; Honda et al., 1995), and in excised plasma membrane patches from bullfrog olfactory neurons (Suzuki, 1994).

The demonstration of plasma membrane $InsP_3$-gated channels in vertebrate olfactory receptor neurons provides evidence consistent with a mediatory role of $InsP_3$ in olfactory transduction. However, it is important to emphasize that the demonstration of $InsP_3$-gated plasma membrane channels in olfactory neurons is not conclusive evidence for the role of these channels in olfactory transduction. In particular, it will be necessary to determine whether these channels are found in olfactory cilia, as suggested by previous calcium imaging experiments in *Xenopus* olfactory neurons (Schild et al., 1995), by immunohistochemical studies of the distribution of $InsP_3$ receptor in rat olfactory epithelium (Cunningham et al., 1993; Kalinoski et al., 1993), and by the fact that $InsP_3$-gated channels with virtually the same characteristics are found in the dendrite of lobster olfactory receptor neurons (Hatt and Ache, 1994). In addition, evidence against a mediatory role for $InsP_3$ (Brunet et al., 1996) must be addressed to determine conclusively what role $InsP_3$ plays in vertebrate olfactory trans-

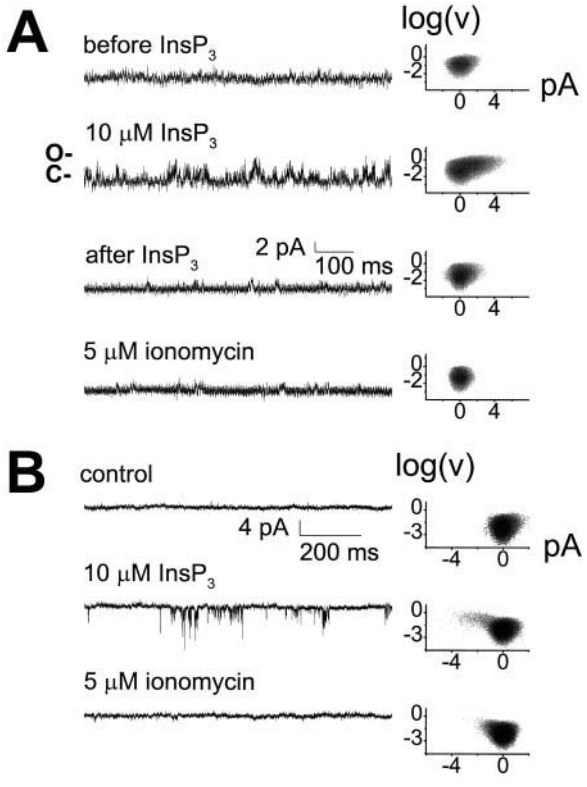

FIGURE 7 Lack of an effect of 5 μM ionomycin on current fluctuations in excised patches from rat olfactory neuron plasma membrane. Holding potential, +60 mV. (*A*) Effect of ionomycin in a patch containing multiple small-conductance $InsP_3$-gated nonspecific cation channels. The bath solution was exchanged successively from $I_{K\text{-}asp}$ (control) to $I_{K\text{-}asp}$ containing 10 μM InsP3, to $I_{K\text{-}asp}$, to $I_{K\text{-}asp}$ with 5 μM ionomycin. C and O denote closed and open states, respectively. (*B*) Effect of ionomycin on a patch containing the rapidly fluctuating $InsP_3$-gated conductance. The bath solution was exchanged successively from $I_{K\text{-}asp}$ (control) to $I_{K\text{-}asp}$ containing 10 μM InsP3 to $I_{K\text{-}asp}$ with 5 μM ionomycin. Notice that in neither figure was ionomycin able to induce current fluctuations similar to the fluctuations induced by $InsP_3$. Lack of an effect of ionomycin was found in four independent experiments. Mean variance histograms corresponding to each trace are shown on the right. The MV histograms for the traces in *A* were calculated for a period of 60 s, and the histograms for the traces in *B* were for periods of 20 s. The number of points with mean and variance falling within each bin is denoted by a 32-step logarithmic gray scale (white = 1, black = 1000).

TABLE 1 Summary of properties of plasma membrane $InsP_3$-gated channels from rat olfactory neurons

	Small conductance nonspecific cation channel	Large conductance nonspecific cation channel	Rapidly fluctuating conductance
Chord conductance (pS)	16 ± 1.7 (10)	64 ± 4 (4)	N/D
Reversal in Ringer's/ Pseudointracellular (mV)	−11.7 (1)	−19 ± 4 (3)	73 ± 4 (4)
Flickering	No	Bursting behavior with flickering, especially at negative potentials	Rapid fluctuations, unitary current events not apparent, 1/f noise spectrum
t_{open} (ms)	25.7 ± 6 (7)	1.6 ± 0.3 (3); 12.6 ± 1.2 (3); 64–130 (2)	N/D
t_{closed} (ms)	12.9 ± 0.8 (7); 83 ± 14 (4); 400 ± 54 (7)	N/D	1.4; 17; 273
Subconductance levels	2×	0.5×	Unitary events not apparent

duction. Finally, there is little information identifying the currents stimulated by odorants thought to stimulate $InsP_3$ production (Miyamoto et al., 1992b; Morales et al., 1994; Kashiwayanagi, 1996). Identification of the conductance underlying the response to these odors as an $InsP_3$-modulated conductance is necessary to conclusively demonstrate the role of $InsP_3$ in olfactory transduction.

The finding of a rapidly fluctuating $InsP_3$-gated conductance with a reversal potential of +74 mV in the presence of Ringer's solution in the pipette and pseudointracellular solution in the bath is novel (Fig. 4). The reversal indicates that the conductance is not a nonspecific cation conductance, but rather that it is selective for sodium and/or calcium over potassium. The rapidly fluctuating conductance did not display discernible unitary current events (Fig. 4 *A*). However, the $1/f$ dependence of the power density spectrum for the excess noise generated by the addition of $InsP_3$ in patches containing this conductance (Fig. 4 *E*) and the fact that the traces possess long "shut" periods (Fig. 4 *A*) are compatible with mediation of this response by channels undergoing conductance fluctuations (DeFelice, 1981; Neher and Stevens, 1977), or with a channel with a dispersion in activation energies caused by the existence of multiple conformational substates (Dewey and Bann, 1992). Previous simultaneous measurements of whole-cell current and intracellular calcium in *Xenopus* olfactory receptor neurons indicated that $InsP_3$ stimulates a calcium-permeable conductance (g_{Ca}) localized to the apical compartments (cilia and olfactory knob) of the neuron (Schild et al., 1995). g_{Ca} displays roughly the same reversal potential as the $InsP_3$-gated rapidly fluctuating conductance shown in Fig. 4. However, it is not clear whether the $InsP_3$-gated conductance shown in Fig. 4 is g_{Ca}. This question must be explored in future experiments.

Strict comparison of single-channel conductance with the $InsP_3$-gated channel of internal stores is not possible because measurements have not been performed under identical conditions. However, it interesting that the $InsP_3$-gated channel found in the ER in cerebellum and in SR in aortic smooth muscle displays openings to multiple conductance levels resembling the behavior of the small and large conductance $InsP_3$-gated nonspecific cation channels described in this manuscript. The conductance of the $InsP_3$-gated channel in smooth muscle SR was first thought to be ~10 pS (Ehrlich and Watras, 1988). However, later work with $InsP_3$ receptor from ER membranes from canine cerebellum (Watras et al., 1991) determined that the channel exists in a fully open state of 80 pS with subconductance levels of 60, 40, and 20 pS (with 50 mM Ba^{2+} as the current carrier). The earlier reports of 10 pS for the conductance of the channel most likely result from openings of the channel to subconductance levels, because in some instances only the small conductance levels are apparent (Ehrlich and Watras, 1988; Watras et al., 1991). The conductance of the small (16 pS) and large (64 pS) conductance $InsP_3$-gated nonspecific cation channels described in this study are on the same order of magnitude of the conductance of the smallest subconductance level and the fully open conductance of the ER $InsP_3$-gated channel (Watras et al., 1991). In addition, the magnitude of the large conductance is four times the magnitude of the small conductance in both cases, and the small conductance and large conductance channels display, respectively, subconductance levels twice and half that of the main level. Therefore, comparison of the olfactory $InsP_3$-gated channel from olfactory neurons with the ER channel suggests the small and large conductance olfactory $InsP_3$-gated channels are not necessarily different molecular entities. It is possible that, as postulated for the ER channel, the two conductance levels detected upon addition of $InsP_3$ to excised patches in this study arise from openings of the same channel protein. Indeed, in studies with isolated catfish olfactory cilia, we have found some records where four conductance levels can clearly be discerned (Teeter and Restrepo, unpublished observations). Resolution of this issue must await experiments with cloned olfactory $InsP_3$ receptor channels.

The similarity of the magnitude of conductance levels for the olfactory $InsP_3$-gated and the cerebellar ER and smooth muscle SR $InsP_3$ receptors suggests that the $InsP_3$ receptor proteins in cerebellum and olfactory neurons may be iden-

tical. Indeed, antibodies recognizing cerebellar $InsP_3$ receptor label olfactory cilia (Cunningham et al., 1993; Kalinoski et al., 1993) and enhance the response of inside-out patches from cultured lobster olfactory neurons to $InsP_3$. However, there are clear differences between the olfactory and ER/SR $InsP_3$-gated nonspecific cation channels because ruthenium red, an inhibitor of ryanodine-sensitive channels in ER and SR, inhibits the olfactory channel but does not inhibit the ER channel (Bezprozvanny and Ehrlich, 1994; Ehrlich and Watras, 1988; Lai et al., 1988; Bezprozvanny et al., 1991; Llano et al., 1994; Khodakhah and Armstrong, 1997). In addition, the ER channel does not display the characteristic flickery bursts of the olfactory channel. These observations and previous studies indicating differences in the effectiveness of $InsP_3$ analogs (Restrepo et al., 1992; Schild et al., 1995) and of labeling of olfactory cilia membranes with radioactive $InsP_3$ analogs (Kalinoski et al., 1992; Restrepo et al., 1992) suggest that there are molecular differences between the cerebellar and olfactory $InsP_3$ receptors. This difference may be a structural difference due to the presence of a different type of $InsP_3$ receptor or a splice variant (Furuichi et al., 1994; Mikoshiba, 1993; Striggow and Ehrlich, 1996) in the olfactory neurons, or it may simply be a difference in posttranslational modification or regulation of the olfactory $InsP_3$ receptor.

Because of the similarity between the ER/SR $InsP_3$ receptor channels and the olfactory small and large conductance channels, it might be thought that the olfactory channels are $InsP_3$-gated channels from ER membranes that fuse with the plasma membrane upon patch excision. However, the pharmacological and biophysical differences, particularly the difference in ruthenium red sensitivity between the ER and olfactory channels, make this possibility highly unlikely. In addition, ER membranes possess a large conductance anion channel that is thought to be involved in maintaining electroneutrality during Ca^{2+} release (Clark et al., 1997). If ER membranes were incorporated into the excised patches in our experiments, a substantial number of patches should display spontaneous current fluctuations mediated by the ER anion channel. We never observed spontaneous current fluctuations with Cs^+ in the bath ($n = 9$). This argues against fusion of ER membranes into the excised patches.

In contrast with the $InsP_3$-gated nonspecific cation conductances, the rapidly fluctuating $InsP_3$-gated conductance shown in Fig. 4 displays kinetics, ion selectivity, and ruthenium red pharmacology that are totally different from those of the ER $InsP_3$-gated channel. The rapid fluctuations are reminiscent of the fluctuations found in the calcium release-activated plasma membrane calcium channels found in some nonexcitable cells (I_{crac}) (Zweifach and Lewis, 1993; Hoth and Penner, 1993). However, the rapidly fluctuating conductance found in the present study is clearly not I_{crac}, because it is directly activated by $InsP_3$, because its power density spectrum displays $1/f$ behavior rather than the Lorentzian behavior displayed by I_{crac} (Zweifach and Lewis, 1993), and because ionomycin, which induces release of Ca^{2+} from internal stores, does not elicit current fluctuations in excised patches from rat olfactory neuron plasma membrane (Fig. 7).

In conclusion, we have strong evidence suggesting that olfactory receptor neurons possess plasma membrane $InsP_3$ receptor channels of at least two types. One type is a nonspecific cation channel displaying large and small conductance openings. The olfactory nonspecific $InsP_3$-gated cation channel shares some functional similarities with but is different from the ER $InsP_3$-gated channel of cerebellum. The other type is a rapidly fluctuating conductance that is not a nonspecific cation channel. It is interesting that the only other study of $InsP_3$-gated plasma membrane calcium channels in a neuron (cerebellar Purkinje cells) reported small and large conductance channels as well as currents composed of rapid fluctuations of various amplitudes (Kuno et al., 1994). In addition, there is biochemical evidence for a plasma membrane $InsP_3$-gated channel present in presynaptic plasma membranes in nerve terminals in a variety of neuronal tissues (Ueda et al., 1996). A strict comparison between our work and the study of Purkinje cells (Kuno et al., 1994) is not possible because of the different ionic conditions, and because the properties of the $InsP_3$-gated plasma membrane channels in Purkinje cells were not described in detail. However, taken together, these results suggest that plasma membrane $InsP_3$-gated channels play a role in neuronal function. Further research is necessary to elucidate this role and, in particular, to determine whether the $InsP_3$-gated channels described in this study play a mediatory role in olfactory transduction.

This work was supported by grant DC00566 from the National Institute of Deafness and Communicative Disorders, National Institutes of Health, and by a grant from the Human Frontier Science Program.

REFERENCES

Bezprozvanny, I., and B. E. Ehrlich. 1994. Inositol 1,4,5-trisphosphate-gated Ca channels from cerebellum: conduction properties for divalent cations and regulation by intraluminal calcium. *J. Gen. Physiol.* 104: 821–856.

Bezprozvanny, I., J. Watras, and B. E. Ehrlich. 1991. Bell-shaped calcium response curves of Ins(1,4,5)- and calcium-gated channels from endoplasmic reticulum. *Nature.* 351:751–754.

Boekhoff, I., W. C. Michel, H. Breer, and B. W. Ache. 1994. Single odors differentially stimulate dual second messenger pathways in lobster olfactory receptor cells. *J. Neurosci.* 14:3304–3309.

Bruch, R. C. 1996. Phosphoinositide second messengers in olfaction. *Comp. Biochem. Physiol. Biochem. Mol. Biol.* 113B:451–459.

Brunet, L. J., G. H. Gold, and J. Ngai. 1996. General anosmia caused by a trageted disruption of the mouse olfactory cyclic nucleotide-gated cation channel. *Neuron.* 17:681–693.

Chan, K. W., N. Langan, J. L. Sui, J. A. Kozak, A. Pabon, J. A. Ladias, and D. E. Logothetis. 1996. A recombinant inwardly rectifying potassium channel coupled to GTP-binding proteins. *J. Gen. Physiol.* 107:381–397.

Clark, A. G., D. Murray, and R. H. Ashley. 1997. Single-channel properties of a rat brain endoplasmic reticulum anion channel. *Biophys. J.* 73: 168–178.

Cunningham, A. M., D. K. Ryugo, A. H. Sharp, R. R. Reed, S. H. Snyder, and G. V. Ronnett. 1993. Neuronal inositol 1,4,5-trisphosphate receptor localized to the plasma membrane of olfactory cilia. *Neuroscience.* 57:339–352.

DeFelice, L. J. 1981. Introduction to Membrane Noise. Plenum Press, New York.

Dempster, J. 1993. Computer Analysis of Electrophysiological Signals. Academic Press, London.

Dewey, T. G., and J. G. Bann. 1992. Protein dynamics and 1/*f* noise. *Biophys. J.* 63:594–598.

Ehrlich, B. E., and J. Watras. 1988. Inositol 1,4,5-trisphosphate activates a channel from smooth muscle sarcoplasmic reticulum. *Nature.* 336: 583–586.

Fadool, D. A., and B. W. Ache. 1992. Plasma membrane inositol 1,4,5-trisphosphate-activated channels mediate signal transduction in lobster olfactory receptor neurons. *Neuron.* 9:907–918.

Fanger, C. M., A. Zweifach, R. E. Dolmetsch, M. Hoth, and R. S. Lewis. 1997. Function follows form: the role of store-operated calcium channels in T-cell activation. *Cell. Physiol. Biochem.* 7:203–218.

Firestein, S. 1996. Scentsational ion channels. *Neuron.* 17:1–2.

Firestein, S., B. Darrow, and G. M. Shepherd. 1991. Activation of the sensory current in salamander olfactory receptor neurons depends on a G protein-mediated cAMP second messenger system. *Neuron.* 6:825–835.

FitzGerald, L., Y. Okada, D. L. Kalinoski, C. DellaCorte, J. G. Brand, J. H. Teeter, and D. Restrepo. 1993. Role of IP_3 in olfactory transduction. *In* Olfaction and Taste XI. K. Kurihara and N. Suzuki, editors. Springer-Verlag, Tokyo. 135–138.

Furuichi, T., K. Kohda, A. Miyawaki, and K. Mikoshiba. 1994. Intracellular channels. *Curr. Opin. Neurobiol.* 4:294–303.

Gomez, M., and E. Nasi. 1996. Ion permeation through light-activated channels in rhabdomeric photoreceptors. *J. Gen. Physiol.* 107:715–730.

Hamill, O. P., A. Marty, E. Neher, B. Sakmann, and F. J. Sigworth. 1981. Improved patch-clamp techniques for high-resolution current recording from cells and cell-free membrane patches. *Pflügers Arch.* 391:85–100.

Hatt, H., and B. W. Ache. 1994. Cyclic nucleotide- and inositol phosphate-gated ion channels in lobster olfactory receptor neurons. *Proc. Natl. Acad. Sci. USA.* 91:6264–6268.

Hirschberg, B., A. Rovner, M. Lieberman, and J. Patlak. 1995. Transfer of twelve charges is needed to open skeletal muscle Na^+ channels. *J. Gen. Physiol.* 106:1053–1068.

Honda, E., J. H. Teeter, and D. Restrepo. 1995. IP_3-gated ion channels in rat olfactory cilia membrane. *Brain Res.* 703:79–85.

Hosoya, Y., M. Yamada, H. Ito, and Y. Kurachi. 1996. A functional model for G protein activation of the muscarinic K^+ channel in guinea pig atrial myocytes. *J. Gen. Physiol.* 108:485–495.

Hoth, M., and R. Penner. 1993. Calcium-release-activated calcium current in rat mast cells. *J. Physiol. (Lond.).* 465:359–386.

Jorquera, O., R. Latorre, and P. Labarca. 1995. Ion channel classes in purified olfactory cilia membranes: planar lipid bilayer studies. *Am. J. Physiol. Cell Physiol.* 269:C1235–C1244.

Kalinoski, D. L., S. B. Aldinger, A. G. Boyle, T. Huque, J. F. Marecek, G. D. Prestwich, and D. Restrepo. 1992. Characterization of a novel inositol 1,4,5-trisphosphate receptor in isolated olfactory cilia. *Biochem. J.* 281:449–456.

Kalinoski, D. L., C. DellaCorte, L. C. Johnson, and D. Restrepo. 1993. Immunocytochemical localization of IP_3 and G_q in the olfactory neuroepithelium of the rat. *Soc. Neurosci. Abstr.* 19:119.

Kashiwayanagi, M. 1996. Dialysis of inositol 1,4,5-trisphosphate induces inward currents and Ca^{2+} uptake in frog olfactory receptor cells. *Biochem. Biophys. Res. Commun.* 225:666–671.

Khodakhah, K., and C. M. Armstrong. 1997. Inositol trisphosphate and ryanodine receptors share a common functional Ca^{2+} pool in cerebellar Purkinje neurons. *Biophys. J.* 73:3349–3357.

Kleene, S. J., R. C. Gesteland, and S. H. Bryant. 1994. An electrophysiological survey of frog olfactory cilia. *J. Exp. Biol.* 195:307–328.

Kuno, M., N. Maeda, and K. Mikoshiba. 1994. IP_3-activated calcium-permeable channels in the inside-out patches of cultured cerebellar Purkinje cells. *Biochem. Biophys. Res. Commun.* 199:1128–1135.

Lai, F. A., H. P. Erickson, E. Rousseau, Q. Y. Liu, and G. Meissner. 1988. Purification and reconstitution of the calcium release channel from skeletal muscle. *Nature.* 331:315–319.

Larsen, E. H., S. E. Gabriel, M. J. Stutts, S. J. Fullton, E. M. Price, and R. C. Boucher. 1996. Endogenous chloride channels of insect Sf9 cells. *J. Gen. Physiol.* 107:695–714.

Llano, I., R. DiPolo, and A. Marty. 1994. Calcium-induced calcium release in cerebellar Purkinje cells. *Neuron.* 12:663–673.

Lowe, G., and G. H. Gold. 1993. Contribution of the ciliary cyclic nucleotide-gated conductance to olfactory transduction in the salamander. *J. Physiol. (Lond.).* 462:175–196.

Michel, W. C., and B. W. Ache. 1992. Cyclic nucleotides mediate an odor-evoked potassium conductance in lobster olfactory receptor cells. *J. Neurosci.* 12:3979–3984.

Michel, W. C., T. S. McClintock, and B. W. Ache. 1991. Inhibition of lobster olfactory receptor cells by an odor-activated potassium conductance. *J. Neurophysiol.* 65:446–453.

Mikoshiba, K. 1993. Inositol 1,4,5-trisphosphate receptor. *Trends Pharmacol. Sci.* 14:86–89.

Miyamoto, T., D. Restrepo, E. J. Cragoe, Jr., and J. H. Teeter. 1992a. IP_3- and cAMP-induced responses in isolated olfactory receptor neurons from the channel catfish. *J. Membr. Biol.* 127:173–183.

Miyamoto, T., D. Restrepo, and J. H. Teeter. 1992b. Voltage-dependent and odorant-regulated currents in isolated olfactory receptor neurons of the channel catfish. *J. Gen. Physiol.* 99:505–529.

Morales, B., G. Ugarte, P. Labarca, and J. Bacigalupo. 1994. Inhibitory K^+ current activated by odorants in toad olfactory neurons. *Proc. R. Soc. Lond. (Biol.).* 257:235–242.

Nakamura, T., H.-H. Lee, H. Kobayashi, and T.-O. Satoh. 1996. Gated conductances in native and reconstituted membranes from frog olfactory cilia. *Biophys. J.* 70:813–817.

Nakamura, T., K. Tsuru, and S. Miyamoto. 1994. Regulation of Ca^{2+} concentration by second messengers in newt olfactory receptor cell. *Neurosci. Lett.* 171:197–200.

Neher, E., and C. F. Stevens. 1977. Conductance fluctuations and ionic pores in membranes. *Annu. Rev. Biophys. Bioenerg.* 6:345–381.

Okada, Y., J. H. Teeter, and D. Restrepo. 1994. Inositol 1,4,5-trisphosphate-gated conductance in isolated rat olfactory neurons. *J. Neurophysiol.* 71:595–602.

Patlak, J. B. 1993. Measuring kinetics of complex single ion channel data using mean-variance histograms. *Biophys. J.* 65:29–42.

Press, W. H., S. A. Teukolsky, W. T. Vettering, and B. P. Flannery. 1992. Numerical recipes in C. Cambridge University Press, Cambridge, England.

Restrepo, D., T. Miyamoto, B. P. Bryant, and J. H. Teeter. 1990. Odor stimuli trigger influx of calcium into olfactory neurons of the channel catfish. *Science.* 249:1166–1168.

Restrepo, D., J. H. Teeter, E. Honda, A. G. Boyle, J. F. Marecek, G. D. Prestwich, and D. L. Kalinoski. 1992. Evidence for an $InsP_3$-gated channel protein in isolated rat olfactory cilia. *Am. J. Physiol.* 263: C667–C673.

Restrepo, D., J. H. Teeter, and D. Schild. 1996a. Second messenger signaling in olfactory transduction. *J. Neurobiol.* 30:37–48.

Restrepo, D., M. M. Zviman, F. W. Lischka, and J. H. Teeter. 1996b. An algorithm for the construction of idealized current traces. *Biophys. J.* 70:A201 (Abstr.).

Sakmann, B., and E. Neher. 1995. Single-Channel Recording. Plenum Press, New York.

Schild, D., F. W. Lischka, and D. Restrepo. 1995. $InsP_3$ causes an increase in apical $[Ca^{2+}]_i$ by activating two distinct components in vertebrate olfactory receptor cells. *J. Neurophysiol.* 73:862–866.

Schild, D., and D. Restrepo. 1998. Transduction mechanisms in vertebrate olfactory receptor cells. *Physiol. Rev.* 78:429–466.

Sigworth, F. J. 1986. Open channel noise. II. A test for coupling between current fluctuations and conformational transitions in the acetylcholine receptor. *Biophys. J.* 49:1041–1046.

Sigworth, F. J. 1995. Charge movements in the sodium channel. *J. Gen. Physiol.* 106:1047–1051.

Silberberg, S. D., and K. L. Magleby. 1993. Preventing errors when estimating single channel properties from the analysis of current fluctuations. *Biophys. J.* 65:1570–1584.

Striggow, F., and B. E. Ehrlich. 1996. Ligand-gated calcium channels inside and out. *Curr. Opin. Cell Biol.* 8:490–495.

Suzuki, N. 1994. IP_3-activated ion channel activities in olfactory receptor neurons from different vertebrate species. *In* Olfaction and Taste XI. K. Kurihara, N. Suzuki, and H. Ogawa, editors. Springer-Verlag, Tokyo. 173–177.

Ueda, H., S. Tamura, N. Fukushima, T. Katada, M. Ui, and M. Satoh. 1996. Inositol 1,4,5-trisphosphate-gated calcium transport through plasma membranes in nerve terminals. *J. Neurosci.* 16:2891–2900.

Watras, J., I. Bezprozvanny, and B. E. Ehrlich. 1991. Inositol 1,4,5-trisphosphate-gated channels in cerebellum: presence of multiple conductance states. *J. Neurosci.* 11:3239–3245.

Zweifach, A., and R. S. Lewis. 1993. Mitogen-regulated Ca^{2+} current of T lymphocytes is activated by depletion of intracellular Ca^{2+} stores. *Proc. Natl. Acad. Sci. USA.* 90:6295–6299.